JOURNAL OF PROPULSION AND POWER
Vol. 9, No. 5, Sept.–Oct. 1993

Effects of Side-Inlet Angle in a Three-Dimensional Side-Dump Combustor

Ruey-Hor Yen* and Tzu-Hsiang Ko†
National Taiwan University, Taipei 10764, Taiwan, Republic of China

A numerical study is performed on the flowfield in a three-dimensional side-dump combustor with dual opposite side-inlets. Emphasis is given to effects of the side-inlet angle on the flow structures. It is found that the side-inlet angle has a great influence on the recirculation structures which play a decisive role on the combustion characteristics. The larger side-inlet angles are found to strengthen the structures of dome recirculation and cause more fluid to recirculate toward the dome region after it is dumped into the combustor. However, the smaller side-inlet angles are beneficial to the continuous development of the recirculation structures from the dome region, across the entrance region, and further to the downstream of the side-inlet. The effects of the side-inlet angle on recirculations in the dome region or downstream of the side-inlet are both contrary to the situation in two-dimensional cases, which clarifies several points of conflict existing from previous investigations of this aspect. Several important factors related closely to the combustion performance, including the detailed three-dimensional vortex structures, the swirl intensity, and the total pressure loss of the flowfield are also studied to supplement present knowledge with valuable information about the flow characteristics as an aid for the combustor design from the viewpoint of fluid dynamics.

Nomenclature

A = surface area
A_{in} = cross-sectional area at inlet port
$A(X_C^*)$ = cross-sectional area at a given X_C^*
C_{PL} = total pressure loss coefficient
C_μ = coefficient in turbulent model
D_C = combustor diameter
L_d = dome length of combustor
$\dot{m}_{in}$ = inlet mass flow rate
$\dot{m}_r$ = recirculated mass flow rate toward dome region
P = pressure
R_C = combustor radial coordinate
R_C^* = nondimensional combustor radial coordinate, $D_C/2$
$S.I.$ = swirl intensity
T_r = ratio of mean temperature in dome region and jet temperature
U = axial mean velocity
U_r = bulk mean velocity in combustor
V = radial mean velocity
$\mathbf{V}$ = velocity vector
V_j = velocity at inlet port
V_t = total velocity, $\sqrt{U^2 + V^2 + W^2}$
W = azimuthal mean velocity
X_C = combustor axial coordinate
X_C^* = nondimensional combustor axial coordinate $X_C \le 0$; $X_C^* = X_C/L_d$, $X_C \ge 0$; $X_C^* = X_C/D_C$
ε = dissipation rate of turbulence kinetic energy
θ = side-inlet angle
θ_C = combustor azimuthal coordinate
κ = turbulent kinetic energy
μ_l = molecular dynamic viscosity
ρ = fluid density

Introduction

THREE-DIMENSIONAL side-dump combustors have been researched as a possible alternative to the axisymmetrical coaxial dump combustors and are of practical importance in integrated rocket-ramjet (I.R.R.) propulsion systems. There are two different types of side-dump combustors which are designed according to different fuel injection positions. For the first type, fuel is injected from the dome-plate end of the combustor while air is introduced from the side-inlets into the combustor. The flame stabilization in this type is determined by the vortex structure in the dome region of the combustor because this is where the dominant mixing process between fuel and air takes place. The flow in such combustors has been investigated by many researchers[1–6] with numerical or experimental methods. In a study by Choudhury[3] on this type combustor, it was found that there exists an optimum dome length for flame stability, and that the side-inlet angle has minimum influence on combustion performance because the side-inlet angle does not have a great effect on the dome vortex structures; therefore, no changes occur in the mixing process of fuel and air in the different side-inlet angles cases.

For another type of side-dump combustor, addressed in this article, the fuel is not injected from the dome-plate, but is introduced from the side-inlets together with the ram air into the combustor. The dome vortex structure is not so decisive a factor as in the former type because the dome region is not the only region in which the dominant mixing of fuel and air takes place. Other effects—such as whether there exist any recirculation structures at the downstream of the side-inlet, which are highly related to the side-inlet angle—will become more important, especially when the fuel injection position is on the downstream side of the side inlet. Very little has been published on the flowfield in this type of combustor. Stull et al.[7] and Vanka et al.[8] investigated the flowfield characteristics of such a three-dimensional side-dump combustor by varying the position of the dome plate and the angle of the side inlets with both experimental and numerical methods. The experimental results obtained by Stull et al.[7] showed that combustion efficiency was more sensitive to the side-inlet angle than to the dome length. This is the opposite of the situation in the former type combustor because of the different fuel injection positions. Although the results calculated by Vanka et al.[8] agree qualitatively with the water tunnel flow visualization, very little crucial information can be obtained from the velocity vector plots shown in the report. In order

Received Oct. 6, 1992; revision received Feb. 26, 1993; accepted for publication April 2, 1993.
*Professor, Department of Mechanical Engineering.
†Research Assistant, Department of Mechanical Engineering.

to study the effect of the side injection angle, they calculated only two cases, 45 and 60 deg. They found there existed a small recirculation downstream of the side-inlet in the 45-deg case, but the recirculation was considerably diminished in size in the 60-deg case. Therefore, they inferred that for the small side-inlet angle, the recirculation eddy would be stretched further into the domain and become more important. Additionally, if the flow were injected at 90 deg to the combustor, a helical flow pattern with an axis at the center of the cross-stream eddy would be set up with no flow recirculation in the axial direction. However, they did not calculate these cases out. Liou and Wu[9] experimentally investigated the flowfield in a dump combustor similar to Stull and Vanka et al.[7,8] except that the azimuthal angle between the two side inlets was 180 deg, as opposed to 90 deg for Stull and Vanka et al.[7,8] Although their measurements were carried out only at a single side-inlet angle of 60 deg, and most of the data are located on the inlet and impinging planes (θ_C = 90- and 0-deg planes, see Fig. 1), these data are nonetheless very valuable to a computational research to validate a computer code. From their measured data on the inlet plane (θ_C = 90-deg plane), they did not find the aforementioned secondary recirculation zone downstream of the side inlet, which has been found in two-dimensional modeling when the side-inlet angle was equal to or larger than 75 deg. Therefore, they concluded that the experimental results of the three-dimensional flow were consistent with the computational results of two-dimensional flow in this respect. This conclusion hints that the effects of the side-inlet angle on this point for the two- and three-dimensional combustor were consistent, i.e., a larger side-inlet angle would more easily cause the recirculation to occur downstream of the side-inlets. However, this conclusion is obviously contrary to the prementioned inference of Vanka's work.[8] Later, Liou et al.[11] performed calculations for the same combustor by using the algebraic Reynolds stress (ASM) turbulent model, but no details about the effects of the side-inlet angle were mentioned. Recently, Liou et al.[12] reanalyzed their experimental data and recalculated the flowfield by using a κ-ε two-equation turbulent model to describe the relationship between the positions of the stagnation points and the side-inlet angles. Their discussions were based on a simple geometrical relation assuming that the inlet jets impinged on each other in a directly opposing manner. They also discussed the relation between the dome length and the fraction of the mass flow rate recirculated into the dome region, finding an optimum dome length under the similar aforementioned assumption which seems more suitable for two-dimensional flow than three-dimensional flow. Zetterström et al.[13] and Sjöblom[14] also studied the flowfield in a side dump combustor with two or four side-inlets by water tunnel observations and combustion tests. They found[13] that a vane is required on the side-inlet duct to avoid flow separation and to get a stable condition for combustion performance. Additionally, the modification on the fuel injector located in the side inlet duct was also found to change the fuel distribution as the fuel is dumped into the combustor together with ram air from the side inlets.

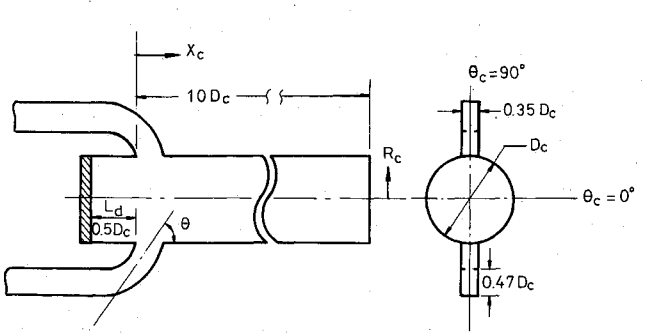

Fig. 1 Geometry and coordinate of the side-dump combustor with dual side-inlets.

The distributions, which are highly related to the side-inlet angle, influenced the flame stability and the combustion efficiency.

The flame stabilization which is expected in the recirculation zones in the combustor, regardless of the recirculation at the dome region or downstream of the dump inlet, is the most important consideration in a dump combustor design. When the fuel is injected into the combustor together with the ram air from the side-inlets, whether and how much fuel and air can be recirculated into the dome region or can be retained in the recirculation zone at the downstream of the side inlets will influence the combustion efficiency and characteristics very significantly.[15,16] In particular, as mentioned by Choudhury,[3] the downstream recirculation will become more and more important when the fuel injection position moves toward the further downstream side of the combustor in the dump inlets. It seems to be very clear that these recirculation structures are very sensitive to the side-inlet angle, but from the literature surveyed above, the factors that affect the recirculation structure have not been studied systematically. Even some inferences about the effects of the side-inlet angle on the recirculation structures at the downstream of the side-inlet made by previous studies are contradictory. In order to obtain a more clear understanding of the flow structures as a prerequisite to the study of the turbulent mixing process of fuel and air, and the reacting flow, further investigation will be worthwhile. This article will study the flowfield in a three-dimensional side-dump combustor with dual opposed side-inlets, with chief emphasis given to the effects of the side-inlet angle on the recirculation structures, which have a decisive influence on combustion characteristics.

Methods

Governing Equations

The dump combustor geometry is conveniently described in the cylindrical polar coordinate system, as shown in Fig. 1. The computational domain excludes the side-inlets, and the inlet conditions at the combustor entrance will be prescribed before solving the flow in the combustor. Since the flow consists of complicated three-dimensional recirculation, the fully elliptic three-dimensional Navier-Stokes equation will be solved. For simplicity, the flow is assumed to be incompressible, isothermal, and steady state in the mean. The time-averaged equations for conservation of mass and momentum can be expressed in the tensor form as follows:

$$\frac{\partial U_i}{\partial x_i} = 0 \tag{1}$$

$$\frac{\partial}{\partial x_j}(\rho U_i U_j) = -\frac{\partial P}{\partial x_i} + \frac{\partial}{\partial x_j}\left[\mu_t\left(\frac{\partial U_i}{\partial x_j} + \frac{\partial U_j}{\partial x_i}\right) - \rho\overline{u_i u_j}\right] \tag{2}$$

In the momentum equation, the body force has been neglected, and the term $-\rho\overline{u_i u_j}$ stands for the Reynolds stress which must be modeled to close the above equation set.

Turbulence Model

It will be shown later that the simple standard κ-ε model and the delicate ASM may both give reasonable mean velocities compared with experiments. However, since the ASM model requires much more computing time than the κ-ε model, the standard κ-ε model is therefore employed in this article. All constants appearing in the turbulent model are given values recommended by Launder and Spalding.[17]

Boundary Conditions

The boundary conditions must be prescribed before solving the above equations. They are given as follows (Fig. 1):

1) Symmetric planes (θ_C = 0 deg and θ_C = 180 deg): $\partial U/\partial\theta_C = \partial V/\partial\theta_C = \partial\kappa/\partial\theta_C = \partial\varepsilon/\partial\theta_C = 0$; $W = 0$.

2) Central axis (Rc = 0): $\partial U/\partial R_C = \partial\kappa/\partial R_C = \partial\varepsilon/\partial R_C = 0$; $V = W = 0$.

3) Exit: The outlet boundary condition is usually assumed to be fully developed, i.e., $\partial U/\partial X_C = \partial V/\partial X_C = \partial W/\partial X_C = \partial\kappa/\partial X_C = \partial\varepsilon/\partial X_C = 0$. However, the condition must be taken with caution, depending on whether the computational domain is long enough to let the flow become developed. Numerical tests have been performed by using $7D_C$, $10D_C$, $15D_C$ as the combustor length. It is found the differences of the axial velocity along the combustor axis results from the cases with combustor lengths as $10D_C$, and $15D_C$ are limited under 5%. This implies $10D_C$ is long enough to adopt the fully developed condition at the exit, so all cases in the present study will adopt $10D_C$ as the combustor length.

4) Inlet: For one basic running case which was performed to validate the computer program by comparing the numerical and experimental results, the conditions for U, V, κ are all taken from the measured data of Liou and Wu.[18] However, since the ε data cannot be obtained from measurements, the ε at inlet was estimated from the relation $\varepsilon_{in} = C_\mu\kappa_{in}^{3/2}/0.03R_C$ according to Khalil et al.[19] The remaining cases for the parametric study adopt the uniform inlet conditions because of the lack of the experimental data. The conditions are $U_{in} = V_j \cos\theta$, $V_{in} = -V_j \sin\theta$, $W_{in} = 0$, $\kappa_{in} = 0.003(U_{in}^2 + V_{in}^2 + W_{in}^2)$, $\varepsilon_{in} = C_\mu\kappa_{in}^{3/2}/0.03\ R_C$, where V_j is the inlet velocity at the combustor entrance. The above adoptions about the inlet conditions of κ and ε are according to Khalil et al.[19] Although the inlet conditions will influence the quantitative results, the qualitative trend will be kept the same. Besides, in practical applications a vane is usually equipped in the side-inlet duct to avoid the flow separations which will make the flow become nearly uniform at the combustor entrance.[13]

5) Walls: Nonslip conditions are employed on all solid walls, but to avoid the need for detailed calculation in the near wall region, where very fine grid is necessary to resolve the steep change of the flow properties, the wall function is applied to bridge the viscous sublayer and the fully turbulent zone.[17]

Numerical Method

The above partial differential equations along with the boundary conditions can be converted into a set of nonlinear algebraic equations by integrating every physical variable over its own control volume which is formed by the grid system. A staggered grid system is adopted in the present study, and the finer grid size has been arranged in the domain with the steep gradient. The power-law scheme[20] is used to formulate the total flux across the faces of the control volumes, including the convective and diffusive terms. The SIMPLEC algorithm[21] is employed to solve the equation set. The convergent criteria in the present study is set as the normalized total overall residue in the whole solution domain of all unknowns, including mass, U, V, W, κ, and ε is less than 5×10^{-4}. The grid independent tests have been performed by using the grid sizes, $45 \times 20 \times 15$, $56 \times 20 \times 15$, $56 \times 32 \times 15$, and $60 \times 20 \times 25$, in X_C, R_C, θ_C direction, respectively. The discrepancy of the axial velocity component at the combustor axis solved by the latter three grid sizes is no more than 4%. Besides, the distributions of axial velocity calculated from the grid sizes of $56 \times 20 \times 15$ and $60 \times 20 \times 25$ were shown in Figs. 2a and 2b (the comparison between the results from different turbulence models in these figures will be discussed later), from which one can see very limited differences existing between the results. Nonetheless, since a large amount of computer resources are required, a thorough grid independence check in all of the three directions was not performed. However, the densities of the grid systems $56 \times 20 \times 15$ and $60 \times 20 \times 25$ are comparable with those used in other studies on the similar problems.[8,11] Consequently, the grid system $56 \times 20 \times 15$ is believed to be sufficient to capture the main flow characteristics considered, and therefore, is chosen for the present study.

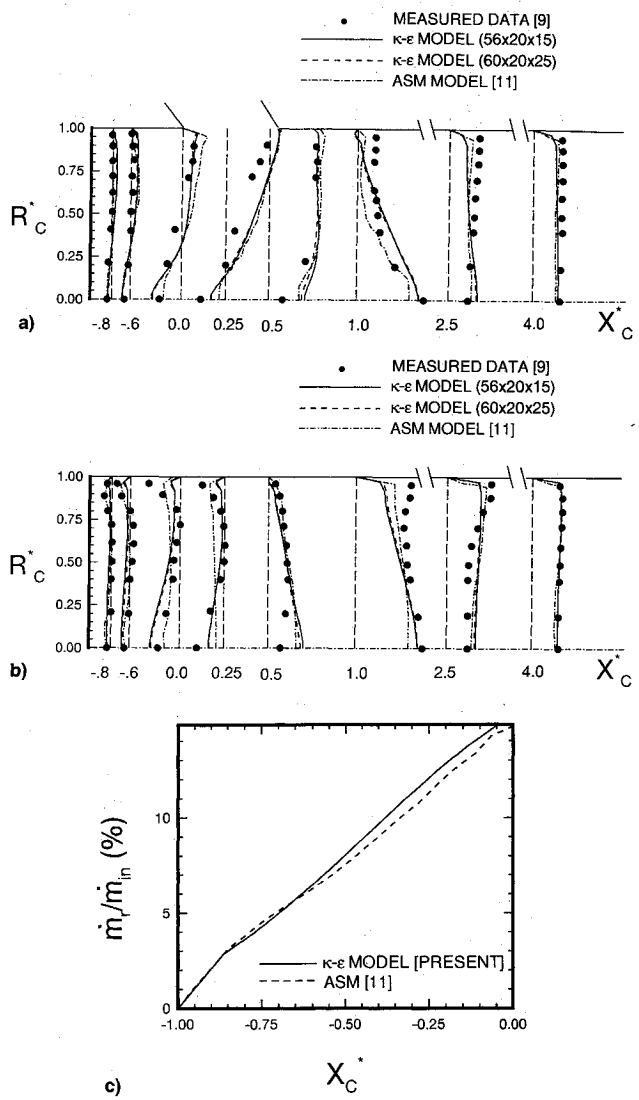

Fig. 2 Comparisons between the calculated and measured axial velocity on a) θ_C = 90-deg plane, b) θ_C = 0-deg plane, and c) recirculated mass flow rate in the dome region calculated by different turbulent models.

Results and Discussion

The geometry of the side-inlet dump combustor for the present study is similar to the case investigated experimentally by Liou and Wu,[9] which is shown in Fig. 1. The dome length is kept as $0.5D_C$, and the axial positions of the side-inlets is located at X_C^* = 0–0.54 for all calculated cases. Since the main stress is focused on the effects of the side-inlet angles on the flow structures, the calculations include θ = 30-, 45-, 60-, 75-, and 90-deg cases. The inlet velocities are the same for all cases. The Reynolds numbers based on the combustor diameter and the bulk mean velocity are between 1.5×10^4 and 3.0×10^4. Because of the symmetric relation, the following discussions are presented on only one-half of the combustor, i.e., the flowfield in the region 0 deg $< \theta_C <$ 180 deg.

Figures 2a–c present the numerical results of a basic running case by using the experimental data near the exit of the side-inlet duct as the combustor entrance conditions to validate the accuracy of the computer code. For this case, the side-inlet angle is 60 deg. The inlet Reynolds number is about 2.6×10^4. Figures 2a and 2b show the distributions of the

axial velocity component on the inlet (θ_C = 90 deg) and the impinging (θ_C = 0 deg) planes, respectively. The figures show fair agreement between the numerical and the experimental results, except that some large discrepancies exist near the combustor entrance regions. These discrepancies have been attributed to the fact that inlet data employed in the calculation are not exactly the same as the real conditions at the combustor entrance.[11] Since experimental results[18] show there exist very complicated secondary flows at the exit of the side-inlet ducts and the data cannot be measured at the exact combustor entrance due to some experimental difficulties,[18] the inlet conditions employed in the calculation were not measured at the combustor entrance but on the top planes near the exit of the side-inlet duct. The numerical results of Liou et al.[11] calculated by ASM turbulent model are also included in the figures for comparison purposes. It is found the κ-ε model is comparable with the ASM model in predicting the average flowfield of the combustor. The distribution shown in Fig. 2c is the fraction of the mass flow rate recirculating toward the dome region along the combustor axis, which is a very important characteristic in flows with swirls and recirculation. It is found that the discrepancies between the results predicted by the simpler κ-ε model and the results predicted by the more complicated ASM model are very limited. Therefore, the κ-ε model is believed to be good enough to capture the correct flow characteristics in such flowfields. A recent study of Liou et al.[22] on the similar problem has arrived at the same conclusion.

Flow Structures in the Combustor

Figures 3a and 3b show the calculated flowfield of the θ = 90- and 30-deg cases. The upper parts of the figures show the three-dimensional velocity vector plots, and the lower parts show the contours of the axial velocity component. The important flow characteristics consist of the vortex structures in the dome region and those at the downstream of the side-inlets. When the flow structures in the dome region are examined from the velocity vector plots in the case of θ = 90 deg, and as shown in the Fig. 3a, the fluids near the jet in the dome region are found to be driven to flow forward to the downstream by the shear force induced by the jets from the side-inlets. However, due to the impingement and impediment of the jet flows, they are forced to recirculate toward the dome plate from the central regions of the combustor, and then to flow out toward the downstream from the outer regions due to the obstructions of the dome plate. A pair of vortices with three-dimensional structures counter-rotate spirally in the dome region and become weaker gradually as they move close to the dome plate. The calculated flow characteristics in the dome region match well with the descriptions in an experimental study by Liou and Wu.[9] For the case of θ = 30 deg as shown in Fig. 3b, the three-dimensional vortex structures in the dome region are not so obvious as in the larger side-inlet angle case, since the impeding and the impinging effects of the dual jets become much weaker in the smaller side-inlet angle cases. It is also noticed that the fluids recirculate to the dome region from the combustor perimeter region in this case, which is different from the θ = 90-deg case.

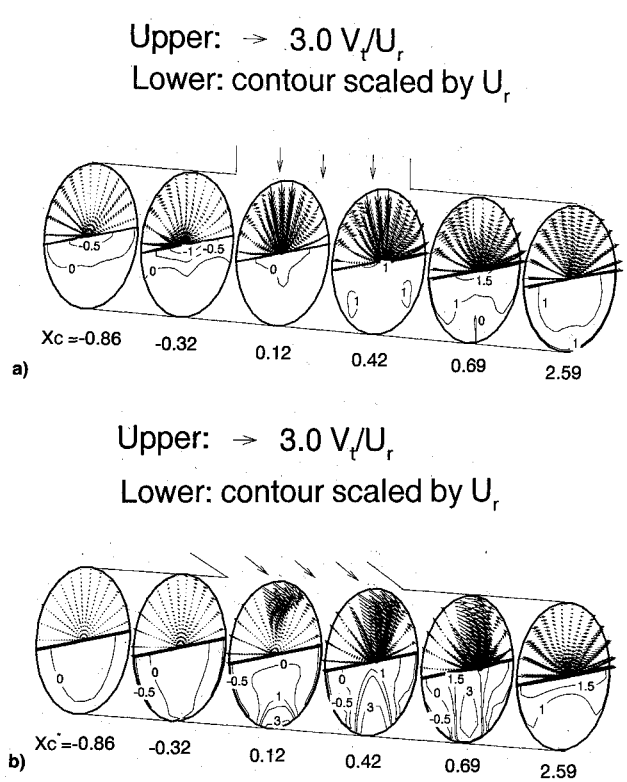

Fig. 3 Three-dimensional velocity vector plots and axial velocity contours: a) θ = 90 deg and b) θ = 30 deg.

The investigations of the flowfield at the downstream of the side-inlets show some different vortex structures from those in the dome regions. Widely extended recirculation zones are found in the θ = 30-deg case, which are indicated by the negative axial velocity in Fig. 3b. But only a very small recirculation zone exists at the positions immediate downstream of the side-inlet (X_C^* = 0.69) in the θ = 90-deg case (Fig. 3a). The different phenomena are observed from the distributions of the velocity components in the axial and radial directions of the side jets with different inlet angles. For the smaller side-inlet angle cases, e.g., θ = 30 deg, the shear driving effects of the jet can stretch toward the position further downstream because of the large axial momentum of the jet. Additionally, when the jet flows with small side-inlet angles are injected into the combustor, there are strong axial convections near the regions of the inlet plane in which the high-pressure field also exists due to the impingement between the dual counter-rotating spiral vortices, the axial recirculation structures do not appear on the inlet plane itself, but distribute in the azimuthally neighboring regions of the inlet plane. This is one of the important characteristics in the three-dimensional flow and is worthy of special attention when studying the three-dimensional recirculation structures at the downstream of the side-inlets. The weak spiral motion with wide axial recirculation zones in this small side-inlet angle case, which is the result of the small and large velocity components of the jets in the radial and axial directions, respectively, makes the three-dimensional vortex with recirculation structures move along an axis inclined at an angle with the combustor axis. Furthermore, in the small side-inlet angles cases, the impingements between the jets with the small radial velocity component are not violent enough to separate the recirculation zones at the downstream of the side-inlet from those in the dome region, so a wide recirculation zone can continuously extend from the dome region to the side-inlet downstream. The flow characteristics can be found from the vector plots in the θ = 30-deg case. As in the large side-inlet angle case, e.g., the case with θ = 90 deg shown in Fig. 3a, the shear driving effects of the inlet jets without any axial velocity component, but with large radial velocity component into the combustor, will result in very limited fluids at the immediate downstream regions of the side-inlet to recirculate in the axial direction. A pair of strong three-dimensional vortices caused by the large radial velocity component of the inlet jet counter-rotate spirally in the combustor along an axis nearly parallel to that of the combustor. The structure is different from that of the small side-inlet angle cases.

Regardless of side-inlet angles, the strength of the three-dimensional vortex motion will gradually decrease as the flow develops along the combustor downstream. Finally, the flow becomes fully developed at some location of the downstream

in the combustor which is obviously related to the side-inlet angles.

Effects of the Side-Inlet Angles on the Recirculation Structures

As pointed by Kennedy,[15] Shaft et al.,[16] and Lefebvre,[23] the recirculation structures have a great effect on the flame blow-off velocities and the averaged residue time of the fuel in the combustor, which both play an important role in determining the combustion characteristics. The different trends of the recirculation structures in θ = 30-deg and θ = 90-deg cases have been pointed out qualitatively in the previous section. The present section will study recirculation structures in more detail in flows with the different side-inlet angles by investigating the axial distributions of the fraction of the recirculated mass flow rate in the combustor quantitatively. From Fig. 4, different recirculation structure patterns are found in the cases with different side-inlet angles. In the dome recirculation structures, the larger side-inlet angle is found to cause the larger fraction of the mass flow rate to recirculate in the region. This is attributed to the more violent impingements and impeding effects of the side jets with larger inlet angles. The present calculated results show the same trend with the experimental formula proposed by Rosenthal[24] which described the relationship between the recirculated mass flow rate and the side-inlet angles in his experimental study on the combustion flow in a three-dimensional side-dump combustor

$$\dot{m}_r/\dot{m}_j = 0.5 \sin \theta T_r^{-0.5} \tag{3}$$

where $\dot{m}_r$, $\dot{m}_j$, θ, and T_r represent the dome recirculating mass flow rate, the inlet mass flow rate of the side jets, side-inlet angle of jet and the ratio of the mean temperature in the dome region, and the jet temperature, respectively. This formula also indicates the larger recirculated mass flow rate in the larger side-inlet angle cases. It is noteworthy that the effects of the larger side-inlet angles in causing the larger recirculated mass flow rate in the dome region of the three-dimensional combustor is opposed to the situation in the two-dimensional axisymmetric combustor,[10] in which the smaller side-inlet angle is found to cause the larger recirculated mass flow rate in the dome region. The differences are attributed to the different flow space for the two- or three-dimensional combustor. Since the flow space for the two-dimensional combustor is limited in the X_C-R_C plane, the larger side-inlet angle (but smaller than 90 deg) will cause the streamline of the inlet jet to turn toward the downstream of the combustor with a larger curvature immediately after being injected into the combustor, which reduces the chance of the fluids recirculating toward the dome region. On the contrary, the flow space in a three-dimensional combustor, including not only the X_C-R_C direction, but also the azimuthal direction, both supply wide flow space. This makes the aforementioned effects of the side-inlet angles on the dome recirculated mass flow rate in the three-dimensional combustor different from those in the two-dimensional combustor. Moreover, the values of the fraction of the recirculated mass flow rate in the dome region are not constants indicating another characteristic of the three-dimensional flows. Figure 4 shows that the maximum of the mass recirculating flow rate in the dome region occurs at about X_C^* = −0.2 for all side-inlet angle cases, and decreases gradually as it nears the dome plate. The maximum fraction among all the cases is about 18%, occurring in the θ = 90-deg case, which is the largest side-inlet angle in the present calculations.

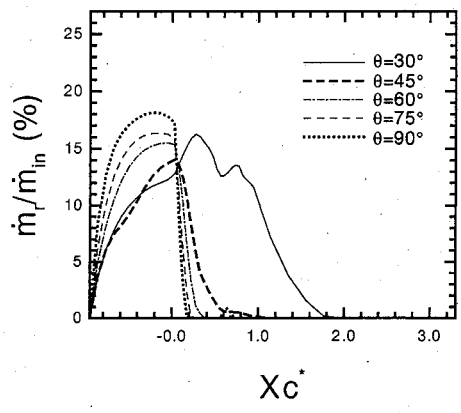

Fig. 4 Axial distributions of the fraction of recirculated mass flow rate.

As for the recirculation structures at the downstream of the side-inlets, wide recirculation zones are found in the cases with the smaller side-inlet angles, including θ = 30- and 45-deg cases, to distribute continuously from the dome region ($X_C^* < 0$), across the side-inlet entrance region (X_C^* = 0–0.54), and then further downstream of the combustor, consistent with previous observations from the velocity vector plots. The recirculation zones stretching from the dome region to the location of X_C^* = 1.8 in the θ = 30-deg case are much wider than those in the θ = 45-deg case, which indicates the smaller side-inlet angles are beneficial to the developments of the recirculation structures further downstream of the combustor. This is due to the fact that much fluid in the wider regions near the jet path will be driven to flow in the X_C-R_C direction by the shear forces induced by the jets with the smaller side-inlet angles and the accompanying larger axial velocity component. Additionally, the recirculations are found from the figure not to be separated with those in the dome regions, since the impingements between the small inlet angle jets with the small radial velocity component are not so violent. Similar effects of the side-inlet angles on the recirculation structures at the downstream of the side-inlets are also found by Schadow and Chiese[2] and Vanka et al.[8] Schadow and Chiese discovered widely stretched recirculation structures at the downstream of the side-inlets in the case with the side-inlet angle equal to 30 deg, while he performed the water tunnel flow visualizations on the isothermal flow in a side-dump combustor with side-inlet angles of 30, 60, and 90 deg. From the combustion tests in the same report, the best combustion efficiency is found to take place in the case with the side-inlet angle of 30 deg, which is also attributed to the existence of the wide recirculation zones which recirculate the hot products toward the upstream and increase the combustion efficiency. In the aforementioned report by Vanka et al.,[8] it was also inferred that the smaller side-inlet angles will be beneficial to the development of recirculation toward the further downstream position of the combustor from his study on the side-inlet angle effects by calculating the flows in θ = 45- and 60-deg cases.

While θ increases above 60 deg, the smaller axial velocity component of the jet flows makes the zones in which the fluids are driven by the shear forces to flow in the X_C-R_C direction become narrower, but the driving effects become strong. The fluids will have a chance to recirculate toward the upstream if an adverse pressure gradient exists. However, the strength of the spiral vortex motion also increases due to the larger radial velocity component of the jets with the larger side-inlet angles. The continuous impingements between the two counter-rotating vortices induce large pressure fields which are detrimental to the formation of the recirculation on the inlet plane near the jet entrance region where the vortex motion is strongest. If the shear driving effects on the fluids to recirculate toward the upstream cannot overcome the large pressure fields, the fluids will be pushed to flow toward downstream, which leads to the three-dimensional vortex motion without the axial recirculation structures. The disappearance of the traces of the recirculation structures at the downstream of the side-inlets in the θ = 60-deg case is an example of the result caused by the above effects. However, when the side-

inlet angle increases to 75 deg, the driving effects on the fluids become stronger and the influenced zone is concentrated more closely to the jet entrance region. Therefore, traces of the recirculation structures can be detected again in the cases from Fig. 4 at the locations immediately downstream of the side-inlets (near $X_C^* = 0.54$). In the $\theta = 90$-deg case, although the distributed regions and the strengths of the recirculation structures become larger than those in the $\theta = 75$-deg case, they are still negligible when compared with the dome recirculation structures. Moreover, the recirculation zones at the downstream of the side-inlet in the cases with larger side-inlet angles have been separated by the strong jets from the dome recirculation. The recirculation structures at the downstream of the side-inlets are more easily developed in the smaller θ cases, which is again opposed to the situations in the two-dimensional axisymmetric cases[10] because of the different flow space in the two- and three-dimensional combustors, mentioned previously. The discovery of the effects of the side-inlet angle on the recirculation structures points out that if the fuel is designed to be injected from the location at the downstream of the side-inlet, jets with small inlet angles must be adopted in order to increase the fuel resident time in the combustor and to obtain the stable flames with the higher combustion efficiency by the widely stretching recirculation structures at the downstream regions.

Effects of the Side-Inlet Angle on the Distribution of Recirculation Zones

Figures 5a and 5b present the distributions of the recirculation zones in the azimuthal direction for the cases of $\theta = 30$ and 60 deg, respectively. In the case of $\theta = 30$ deg, the largest $\dot{m}_r/\dot{m}_{in}$ in the dome region ($X_C^* = -0.682, -0.227$) takes place on the impinging planes ($\theta_C = 0, 180$ deg) where the impingements between the jets are the most violent. The value of $\dot{m}_r/\dot{m}_{in}$ on the inlet plane ($\theta_C = 90$ deg) is always the lowest since most of the fluids near the plane in the dome region are driven to flow toward the downstream. The larger values of $\dot{m}_r/\dot{m}_{in}$ can still be found at $X_C^* = 0.025$ near the inlet plane, which shows the recirculation structure is not

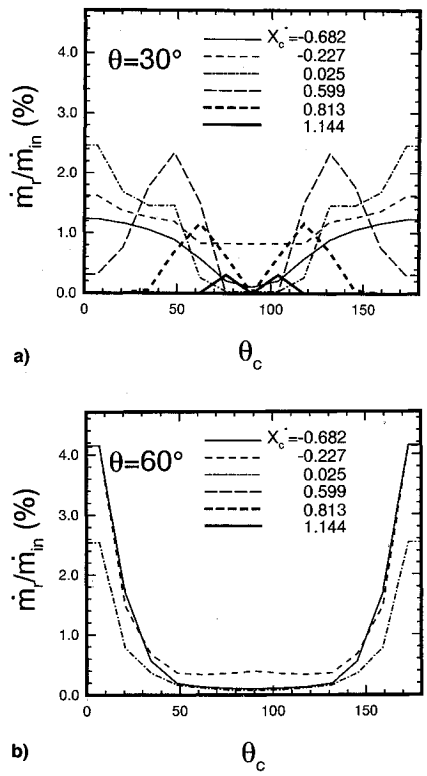

Fig. 5 Azimuthal distributions of the recirculation zones: a) $\theta = 30$ deg and b) $\theta = 60$ deg.

interrupted by the inlet jets at the entrance regions. As the recirculation structures at the downstream of the side-inlet are mentioned ($X_C^* > 0.54$), the maximum of the fraction does not take place on the impinging planes, but always on both sides of the inlet planes, which is consistent with the previous observation from the velocity vector plots. The values of $\dot{m}_r/\dot{m}_{in}$ decreases gradually as the flow develops toward the downstream, and the location of the maximum value of $\dot{m}_r/\dot{m}_{in}$ gradually moves toward the inlet plane; the maximum value of $\dot{m}_r/\dot{m}_{in}$ never appears on the inlet plane itself, however. Figure 5b shows the distribution of $\dot{m}_r/\dot{m}_{in}$ for the case of $\theta = 60$ deg, which is the same condition as the measured case of Liou and Wu.[9] The maximum of $\dot{m}_r/\dot{m}_{in}$ in the dome region still appears near the impinging planes, but their values are larger than those in $\theta = 30$-deg case. Since the dome recirculation zone would be gradually separated by the strong jet flows with the larger side-inlet angles, the values of $\dot{m}_r/\dot{m}_{in}$ at $X_C^* = 0.025$ near the inlet plane which are located in the jet entrance region are smaller than those in $\theta = 30$-deg case. Downstream of the side-inlets ($X_C^* > 0.54$) there are no recirculation structures, which is consistent with the previous discussion and the experimental report in Liou and Wu.[9] However, their inferences[9] about the agreement between the experimental results of the three-dimensional flow in which there is no recirculation structures at the downstream of the side-inlet on the inlet plane, and the computational results of the two-dimensional flow,[10] in which the recirculation will be set up only when $\theta > 75$ deg can very easily give the mistaken impression that the larger θ would more easily cause the recirculation to appear at the downstream of the side-inlets in the three-dimensional combustor, just as the situations in the two-dimensional combustor. Actually, Liou and Wu's experimental investigations, which only performed measurements on the inlet and impinging planes, ignored the fact that the smaller side-inlet angles are beneficial to the development of the recirculation structures on both azimuthal sides of the inlet planes, but not on the inlet plane itself at the downstream of the side-inlets, which has been clearly presented in the present work and is inferred similarly by Vanka et al.[8] Since the recirculation structures at the downstream of the side-inlets has a great influence on combustion characteristics, which has been pointed out by Schadow and Chiese,[2] the contrary effects of the side-inlet angle on the recirculation structures in two- and three-dimensional combustors should be noticed with special caution.

Effects of Side-Inlet Angles on the Swirl Intensity

An understanding of the development of the strength of the three-dimensional vortex motion for the cases with different θ is necessary for combustor design. The *S.I.* is defined in this article to examine the development of the vortex motion:

$$S.I. = \frac{\int_{A(X_C^*)} \frac{1}{2}\rho W^2 |V \cdot dA|}{\int_{A_{in}} \frac{1}{2}\rho (U^2 + V^2 + W^2)|V \cdot dA|} \tag{4}$$

The above definition is similar to that in Liou and Hwang,[11] but the term $(\rho V \cdot dA)$ is changed into its absolute value to avoid cancelling between the positive and negative terms in performing the integrations for the cases with recirculation zones. Figure 6 shows the axial distribution of *S.I.* for different θ cases. It can be found that the larger *S.I.* appears in the larger θ cases, in which a wider space is required for the flow to develop into a unidirection flow pattern. In all cases, the largest *S.I.* takes place as expected at the entrance region of the side-inlets, and decays rapidly to only about one-third of the largest value around the location of $X_C^* = 1.5$. The rapid decay of *S.I.* results from the violent impingements between

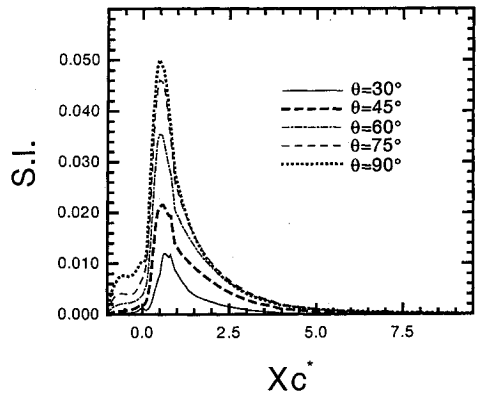

Fig. 6 Axial distributions of swirl intensity.

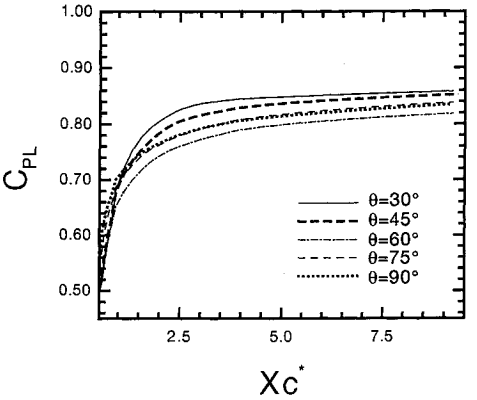

Fig. 7 Axial distributions of total pressure loss coefficient.

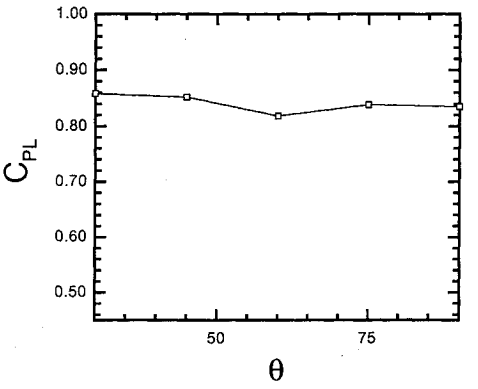

Fig. 8 Total pressure loss coefficient at combustor exit.

the counter-rotating spiral vortices in the combustor, which causes the very steep velocity gradient to transfer the kinetic energy of the mean flow into the turbulent kinetic energy. Since the strong vortex motion is beneficial to the fuel and air mixing, the fast decay of the *S.I.* indicates that the fuel injection position should be arranged as close as possible to the side-inlet, especially when it is designed to be located at the downstream of the side-inlets. Otherwise, the chances to increase the mixing between the fuel and air by using the strong vortex motion will be greatly reduced.

Effects of Side-Inlet Angles on the Total Pressure Loss

The total pressure represents the mechanical energy in the flows. Too large a total pressure loss will reduce the magnitude of specific impulse for a propulsive system. Therefore, from the viewpoint of combustor design, an understanding about how the values of θ to influence the total pressure loss is another important point in addition to the mixing of fuel and air. The total pressure loss coefficient is defined as

$$C_{PL} = \frac{\int_{A_{in}} \left[P + \frac{1}{2}\rho(U^2 + V^2 + W^2) \right] |V \cdot dA|}{\int_{A_{in}} \frac{1}{2}\rho(U^2 + V^2 + W^2)|V \cdot dA|} - \frac{\int_{A(X_C^*)} \left[P + \frac{1}{2}\rho(U^2 + V^2 + W^2) \right] |V \cdot dA|}{\int_{A_{in}} \frac{1}{2}\rho(U^2 + V^2 + W^2)|V \cdot dA|} \quad (5)$$

In the definition the absolute value of $(V \cdot dA)$ is adopted for the same reason as in the definition of *S.I.* Since there is no energy source in the nonreacting flows, the values of C_{PL} in the present calculation cases are all positive. Figure 7 shows the distribution of the C_{PL} for the different θ cases. The trends in all cases are very similar. The steep changes of the values of C_{PL} takes place near the inlet entrance region where the violent impingements between the vortex motion exists to dissipate a lot of the mechanical energy. The changes become more tender and the magnitude of C_{PL} gradually approaches a constant. Figure 8 presents the C_{PL} at the combustor exit for the different side-inlet angle cases, among which the θ = 60-deg case has the smallest value of C_{PL}, indicating the smallest total pressure loss in the case. However, the differences between these cases are very limited, which shows the similar results obtained by Stull et al.[7] and Sjöblom[14] when they investigated the total pressure recovery experimentally in the combustion flow.

Summary and Conclusions

The three-dimensional flowfields in a dual opposite side-inlet dump combustor with various side-inlet angles have been investigated in detail. The important conclusions are as follows:

1) The larger side-inlet angle will strengthen the recirculation and result in a larger fraction of the mass flow rate to recirculate toward the dome region after being injected from the side-inlets. This trend is contrary to the situations in a two-dimensional axisymmetric side-dump combustor due to the different flow space in two- and three-dimensional combustors.

2) The effects of the side-inlet angles on the recirculation structures at the downstream of the side-inlets are very complicated. The smaller side-inlet angle is beneficial to the development of the recirculation zones which are continuously distributed from the dome region, across the inlet entrance, and further downstream of the side-inlet. The strongest recirculation structures do not take place on the inlet plane, but on both of its azimuthally neighboring side regions. This is one of the characteristics of the three dimensional flows and should be taken with special caution when investigating the recirculation structures in a three-dimensional combustor. The recirculation structures do not occur at the downstream of the side-inlet if the side-inlet angle increases to 60 deg. Until its value is larger than 75 deg, the recirculation structures appear again at the immediate downstream region of the side-inlets. But the distributed region and the strength of these recirculations are relatively small compared with the dome recirculation, and are separated by the strong impinging jets from the dome recirculation zones. The recirculation structures in these cases are different from those in the cases with smaller side-inlet angles. The discovery of the relationship between the side-inlet angles and the three-dimensional recirculation structures, which is definitely different from the two-dimensional flow, clarifies conflicting statements made in previous studies.

3) The larger side-inlet angle will increase the swirl intensity of the flow. The strongest vortex motion, as expected, takes place near the downstream of the side-inlet in all calculated cases, and it should be noticed that the intensity diminishes very fast as the vortex motion develops downstream. Only one-third of the largest swirl intensity can be retained at the position of about one combustor diameter downstream of the side-inlet. The fast decay of the swirl motion indicates that if the fuel is designed to be injected at the downstream of the side-inlets, its position should be arranged at the position as immediate as possible to the side-inlet in order to take advantage of the strong swirl motion to increase the mixing of fuel and air.

4) As with similar descriptions by previous studies on the combustion flow in the three-dimensional side-dump combustor, the total pressure losses in the present calculated cold flows are found to be insensitive to the side-inlet angles. Therefore, the considerations about the total pressure loss in determining the side-inlet angle for combustor design are less important.

Acknowledgment

This investigation was supported by the National Science Council, Republic of China through Grant NSC81-0401-E002-584 at National Taiwan University and is gratefully acknowledged.

References

[1]Choudhury, P. R., "Experiments on Multiple Vortices in a Side Dump Gas Generator Ramjet," *Proceedings of the 17th JANNAF Combustion Meeting*, CPIA Publ. 329, Vol. 1, 1980, pp. 481–488.

[2]Schadow, K. C., and Chiese, D. J., "Water Tunnel and Windowed Combustion as Tools for Ducted Rocket Development," *Proceedings of the 18th JANNAF Propulsion Meeting*, CPIA Publ. 340, Vol. 2, 1981, pp. 101–115.

[3]Choudhury, P. R., "Characteristics of a Side-Dump Gas Generator Ramjet," AIAA Paper 82-1258, June 1982.

[4]Chen, L., and Tao, C. C., "Study on the Side-Inlet Dumped Combustor of Solid Ducted Rocket with Reacting Flow," AIAA Paper 84-1398, June 1984.

[5]Cherng, D. L., Yang, V., and Kou, K. K., "Numerical Study of Turbulent Reacting Flows in Solid-Propellant Ducted Rocket Combustors," *Journal of Propulsion and Power*, Vol. 5, No. 6, 1989, pp. 678–685.

[6]Vanka, S. P., Craig, R. R., and Stull, F. D., "Mixing Chemical Reaction and Flow Field Development in Ducted Rockets," AIAA Paper 85-1271, July 1985.

[7]Stull, F. D., Craig, R. R., Streby, G. D., and Vanka, S. P., "Investigation of a Dual Inlet Side Dump Combustor Using Liquid Fuel Injection," *Journal of Propulsion and Power*, Vol. 1, No. 1, 1985, pp. 83–88.

[8]Vanka, S. P., Stull, F. D., and Craig, R. R., "Analytical Characteristics of Flow Fields in Side-Inlet Dump Combustors," AIAA Paper 83-1399, June 1983.

[9]Liou, T. M., and Wu, S. M., "Flowfield in a Dual Inlet Side-Dump Combustor," *Journal of Propulsion and Power*, Vol. 4, No. 1, 1988, pp. 53–60.

[10]Liou, T. M., and Hwang, Y. H., "A Study of Flowfields in a Side-Dump Combustor with Various Dump Angles," *Journal of the Chinese Society of Mechanical Engineers, Transactions of Chinese Institute of Engineers* (in Chinese), Sec. C, Vol. 7, No. 4, 1986, pp. 253–258.

[11]Liou, T. M., and Hwang, Y. H., "Calculation of 3-D Turbulent Flow Fields in Side-Inlet Ramjet Combustors with an Algebraic Reynolds Stress Model," *Journal of Propulsion and Power*, Vol. 5, No. 6, 1989, pp. 686–693.

[12]Liou, T. M., Hwang, Y. H., and Wu, S. M., "The Three-Dimensional Jet-Jet Impingement Flow in a Closed-End Cylindrical Duct," *Journal of Fluids Engineering*, Vol. 112, June 1990, pp. 171–178.

[13]Zetterström, K. A., Sjöblom, B., and Jarnmo, A., "Solid Ducted Rocket Engine Combustor Tests," *Proceedings of the Sixth International Symposium of Air Breathing Engines*, ISABE Paper 83-7001, June 1983, pp. 9–16.

[14]Sjöblom, B., "Full-Scale Liquid Fuel Ramjet Combustor Tests," *Proceedings of the Ninth International Symposium of Air Breathing Engines*, ISABE Paper 89-7027, 1989, pp. 273–281.

[15]Kennedy, J. B., "Ramburner Flow Visualization Studies," *Proceedings of the 11th JANNAF Combustion Meeting*, Vol. 11, Chemical Propulsion Information Agency Pub. 261, 1974, pp. 415–440.

[16]Shaft, M., Goldman, Y., and Greenberg, J. B., "An Investigation of Impinging Jets in Flow with Sudden Expansion," *Proceedings of the 22nd Israel Annual Conference on Aviation and Astronautics*, Israel Ministry of Transport, March 1980, pp. 100–106.

[17]Launder, B. E., and Spalding, D. B., "The Numerical Computation of Turbulent Flows," *Computer Methods in Applied Mechanics and Engineering*, Vol. 3, 1974, pp. 269–289.

[18]Liou, T. M., and Wu, S. M., "Application of Laser Velocimetry to the Curved Inlet Duct of a Side Dump Combustor," Third International Symposium on Application of Laser-Doppler Anemometer to Fluid Mechanics, Lisbon, Portugal, July 1986.

[19]Khalil, E. E., Spalding, D. D., and Whitelaw, J. H., "The Calculation of Local Flow Properties in Two-Dimensional Furnaces," *Internal Journal of Heat and Mass Transfer*, Vol. 18, 1975, pp. 775–791.

[20]Patankar, S. V., *Numerical Heat Transfer and Fluid Flow*, Hemisphere, Washington, DC, 1980, pp. 90–92.

[21]Vandoormaul, J. P., and Raithby, G. D., "Enhancements of the SIMPLE Method for Predicting Incompressible Fluid Flow," *Numerical Heat Transfer*, Vol. 7, 1984, pp. 147–161.

[22]Liou, T. M., Hwang, Y. H., and Chen, L., "Prediction of Confined Three-Dimensional Impinging Flows with Various Turbulence Model," *Journal of Fluids Engineering*, Vol. 114, June 1992, pp. 220–230.

[23]Lefebvre, A. H., *Gas Turbine Combustion*, Hemisphere, Washington, DC, 1983, pp. 126–135.

[24]Rosenthal, J., "Exploring Methods for Determination of Gas Flow and Temperature Pattern in Gas Turbine Combustors," Aeronautical Research Lab., ARL/ME NOTE 235, Australia, 1959.